Adsorption 5, 135–143 (1999)


# A Temperature Frequency Response Method for Adsorption Kinetics Measurements

PH. GRENIER, A. MALKA-EDERY AND V. BOURDIN
*LIMSI-CNRS BP 133 F91403 Orsay, France*
grenier@limsi.fr

**Abstract.** A Frequency Response Method based on the infrared measurement of the sample temperature has been developed for adsorption kinetics measurements. It consists in modulating the experimental chamber volume at constant frequency. The complex ratio of the temperature response over the pressure response is independent of time but is a function of the frequency depending on all the kinetics parameters of the system. This method is accurate and allows to measure very fast kinetics. Its major drawback is that a spurious signal is observed at high pressure in absence of adsorption. The results obtained with silicalite-propane and NaX-carbon dioxide are compared with results obtained from other techniques (NMR, permeation, etc.).

**Keywords:** diffusion, kinetics measurements, frequency response, NaX zeolite, silicalite

## Introduction

To explain the very large discrepancies observed in the past between the diffusivity values derived from measurement by macroscopic (e.g., "gravimetric uptake") and microscopic (e.g., NMR) methods, the influence of extracrystalline mass or heat transfer resistances have been mentioned (Kärger and Ruthven, 1989, 1992). The most important side effects that could perturb a kinetic measurement are:

- the "heat effect" due to the limited heat exchange rate between the crystal and its surroundings (Ruthven et al, 1980; Sun and Meunier, 1987),
- the presence of a surface barrier slowing the mass exchange through the crystal surface (Do, 1989; Kocirik et al., 1990),
- the finite transport rate in the gas phase surrounding the crystal limited either by the macroporous diffusivity, by the intergranular resistance ("bed effect") or by the experimental apparatus itself (Ruckenstein et al., 1971; Van-den-Begin and Rees, 1989; Zhong et al., 1993).

Nevertheless, there are still a number of experimental studies in which the discrepancy cannot be accounted for (Kärger and Ruthven, 1992).

In order to contribute to the resolution of the divergence that remains in certain cases of measurement, we need a macroscopic method covering a large range of time scales, with negligible external mass transfer resistance. This has been achieved by the Thermal Frequency Response (TFR) method.

## Principle of the TFR Method

Consider an adsorbent sample situated in a chamber whose volume varies periodically. The change of the volume induces a change in the pressure. This pressure change induces a change in the adsorbed amount and thus, due to the sorption enthalpy, a change in the sample temperature. When steady state is reached, the volume $V$, the pressure $P$ and the temperature $T$ are periodic functions of time at the same frequency.

Let us consider at first a sinusoidal volume variation at angular frequency $\omega$, whose relative amplitude, $v$, is small enough to ensure system linearity. The pressure change, $\Delta P$, and the temperature change, $\Delta T$, around their mean values, respectively, $P_e$ and $T_e$, may be written:

$$\begin{aligned} \Delta P &= P - P_e = A_P e^{i\omega t} \\ \Delta T &= T - T_e = A_T e^{i(\omega t+\varphi)} \end{aligned} \quad (1)$$

The complex ratio $\Delta T/\Delta P$ is independent of time but depends on the frequency. Thus we define a function characteristic of the system under study:

$$\theta(\omega) = v_0 P_e \frac{\Delta T}{\Delta P} \tag{2}$$

Where $v_0$ is a normalization factor independent of the frequency, close to the mean value of the relative volume amplitude, $v$. Its amplitude $v_0 P_e A_T/A_P$, and phase, $\varphi$, depend on the thermodynamic and kinetic parameters of the adsorbent-adsorbate system. In the real domain that function is split up into an in-phase function and an out-of-phase function.

As the characteristic function is related to the measured pressure variation and not to the volume variation, many spurious effects are eliminated (Bourdin et al., 1996a). Among them the possible adsorption by the chamber wall and the overpressure due to the non isothermal compression of the gas. In the simplest case of a monodispersed crystal sample, the relevant equations of the system are:

Mass balance:

$$\frac{d}{dt}\left(\frac{PV}{RT} + V_s\bar{q}\right) = 0 \tag{3}$$

where $V_s$ is the sample volume and $\bar{q}$ the adsorbate mean concentration.

Heat balance:

$$C_s\frac{dT}{dt} + \frac{(\sigma+1)h}{R_c}\Delta T = |\Delta H|\frac{d\bar{q}}{dt} \tag{4}$$

where $C_s$ is the overall volumetric heat capacity of the sample, $R_c$ is the crystal radius, $\Delta H$ is the specific mass sorption enthalpy and $h$ is the overall heat transfer coefficient from the sample to the surroundings. The different values of the shape parameter of the adsorbent particles $\sigma$ are respectively 0, 1 or 2 for slabs, cylinders or spheres. The temperature is assumed to be uniform owing to the smallness of the crystals.

Diffusion equation:

$$\frac{\partial q}{\partial t}\frac{D_c}{r_c^\sigma}\frac{\partial}{\partial r_c}\left(r_c^\sigma\frac{\partial q}{\partial r_c}\right) \tag{5}$$

where $D_c$ is the diffusion coefficient.

Boundary conditions, taking into account a finite mass transfer rate at the adsorbent surface:

$$\left.\frac{\partial q}{\partial r_c}\right|_{r_c=0} = 0 \quad -D_c\left.\frac{\partial q}{\partial r_c}\right|_{r_c=R_c} = k_s(q|_{r_c=R_c} - q^*) \tag{6}$$

where $k_s$ is the surface barrier transfer coefficient. When the diffusion resistance is negligible ($D_c \gg 1$), the concentration, $q$, inside the pellet is uniform and Eqs. (5) and (6) can be reduced to:

$$\frac{\partial q}{\partial t} = \frac{(\sigma+1)}{R_c}k_s(q - q^*) \tag{7}$$

In that case the model becomes identical to a linear driving force (LDF) model.

The mass that would be adsorbed at equilibrium, $q*(P,T)$, is given by a linearized state equation around its mean value, $q_e$:

$$q^* - q_e = K_P\Delta P - K_T\Delta T \tag{8}$$

$K_P$ and $K_T$ are the slope at the equilibrium point for the isotherm and isobar respectively.

As $V(t)$ is a sinusoidal function of time, these equations yield an explicit complex characteristic function $\theta(\omega)$:

$$\theta(\omega) = A(\omega)e^{i\varphi(\omega)} \tag{9}$$

where $A$ and $\varphi$ are respectively the amplitude and phase lag. In the real domain that function splits up into 2 functions:

$$\theta_{in} = A\ \cos\ \varphi \tag{10}$$

$$\theta_{out} = A\ \sin\ \varphi \tag{11}$$

respectively called in-phase and out-of-phase functions.

Comparing this function to experimental data allows one to identify the heat and mass transfer kinetic parameters, $h$, $D_c$ and $k_s$ (Bourdin et al., 1996b).

For a bidispersed sample with a surface barrier and diffusion at macroporous and nanoporous levels, the equations are more complex but yield an explicit characteristic function as in the case of monodispersed particles.

For any periodic volume variation, the volume can be considered as a sum of harmonic functions. As the amplitude of the volume change is small enough to ensure the system linearity, the previous analysis remains valid.

The frequency response method is extremely effective for measuring small signals accurately. Because the amplitude and phase of the characteristic function, $\theta$, are independent of time, the experimental result is given by averaging a number of data increasing with the

measurement duration. Thus, the experimental errors decrease statistically as $t^{-1/2}$ (where $t$ is the experiment duration). Moreover, the phase lag, $\varphi$, is a fraction of the period and thus, in fact, a time. Thus its measurement is perfectly suited for kinetics experiments.

### Experimental Set Up

The apparatus built at LIMSI for adsorption kinetics measurements is schematically presented on Fig. 1. The adsorbent sample (1) is situated in a chamber closed by bellows (2). A stepper motor (3) and a cam move the bellows at a constant adjustable frequency. A position gauge (4) gives the bellows position and thus the chamber volume. The pressure is measured with a high accuracy, high speed Baratron® pressure gauge (5). This gauge is placed quite close to the sample, in order to avoid any phase lag. The temperature variations are measured with an infrared detector (6) whose response is proportional to the difference between the sample temperature and the temperature of a reference black-body (7).

The relative amplitude of the volume change is less than 2%. This ensures that the system is linear. The profile of the cam actuated by the stepper motor is designed to give the sum of six harmonics of the fundamental frequency, with the same amplitude. Thus six frequencies, covering one decade, are measured simultaneously. The measurements are performed from $10^{-4}$ Hz or less, to 28 Hz.

The infrared temperature measurement presents the following advantages:

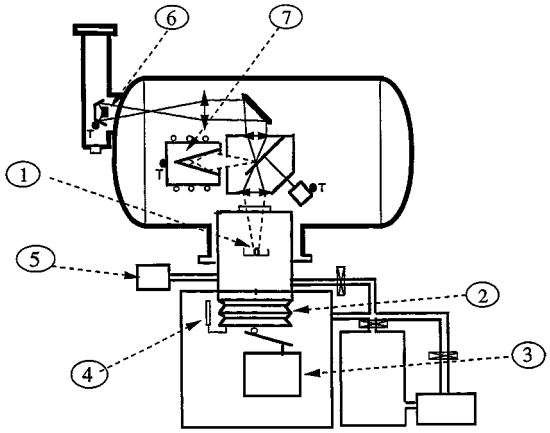


*Figure 1.* Experimental Apparatus. (1): Sample. (2): Bellows. (3): Stepper motor and cam. (4): Position gauge. (5): Pressure gauge. (6): Infrared detector. (7): Reference black body.

- The thermometer is the sample itself. Thus, there is neither difference in amplitude nor any delay between the sample temperature and the measured temperature (except calibration errors).
- No perturbation of the temperature change of the sample occurs, e.g., due to parasitic heat capacity of a temperature gauge or heat flux coming through electrical wires.
- The measurement of temperature is still reliable even for a very small amount of adsorbent crystals when pressure measurements are infeasible.
- The infrared detection is extremely fast and only limited by the associated electronics. The minimum overall time constant of the infrared detection system is 1 ms.
- The sensitivity is excellent. The mean error observed on the temperature amplitude for few seconds recording time is generally less than 0.2 mK.
- The measured temperature is the surface temperature of the adsorbing particles and not their mean temperature. In the case of bidispersed particles, this gives additional information allowing, in many cases, to discriminate macroporous from microporous mass transfer (see below).

### Characteristic Function Properties

The characteristic function, $\theta(\omega)$, is independent of the sample mass, so the sample may be a very thin layer of crystals. The problems due to intergranular diffusion resistance ("bed effect") are eliminated.

First of all, let us describe the typical features of these functions in the frequent case of a sample of monodispersed particles (for instance zeolite crystals of uniform dimension). Each resistance to heat and mass transfer is related to a characteristic time. These characteristic times, for heat exchange between the sample and its surroundings, for mass diffusion, and for surface exchange may be expressed as follows:

$$\tau_{\mathrm{h}} = \frac{(1+\gamma)C_{\mathrm{s}}R_{\mathrm{c}}}{(\sigma+1)h} \tag{12}$$

$$\tau_{\mathrm{D}} = \frac{R_{\mathrm{c}}^2}{(\sigma+1)(\sigma+3)D_{\mathrm{c}}} \tag{13}$$

$$\tau_{\mathrm{s}} = \frac{R_{\mathrm{c}}}{(\sigma+1)k_{\mathrm{s}}} \tag{14}$$

with

$$\gamma = \frac{|\Delta H| K_{\mathrm{T}}}{C_{\mathrm{s}}}$$

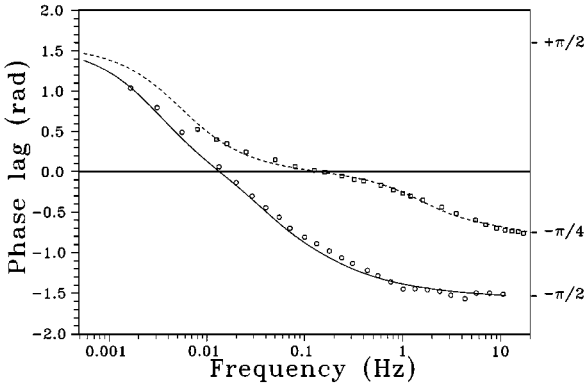


*Figure 2.* Comparison of the phase lag observed with 2 systems: (○)(–): Silicalite-butane at 40 Pa and 300 K, experiment and model, respectively; (□)(---): NaX-butane at 95 Pa and 300 K, experiment and model, respectively. In the first case, surface barrier resistance is dominant and the phase lag tends towards $-\pi/2$ at high frequency. In the second case, Fickian diffusion is dominant and the phase lag tends towards $-\pi/4$. In all cases at low frequency the heat transfer is the limiting effect and the phase lag tends towards $+\pi/2$.

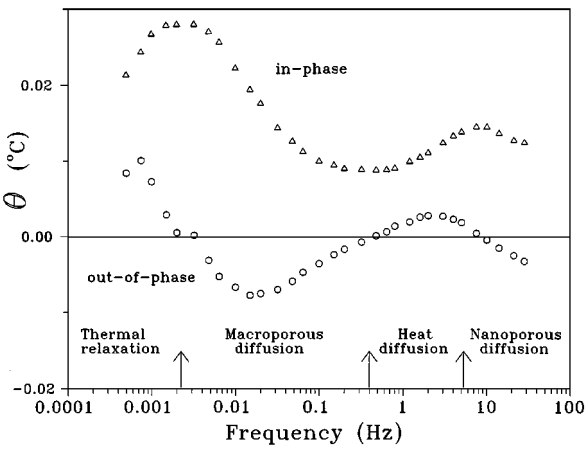


*Figure 3.* Characteristic function obtained with 4A pellets—water system. (Δ): in-phase function; (○): out-of-phase function. Four different domain are clearly visible, separated by the zeros of the out-of-phase function. A dominant heat transfer resistance gives a positive out-of-phase function. A dominant mass transfer resistance gives a negative out-of-phase function.

Typical curves of phase lag, $\varphi$, are shown in Fig. 2. At very low frequency the heat transfer to the wall is important. The system is quasi-isothermal and the phase lag is positive and close to $\pi/2$. When frequency increases the heat transfer to the wall becomes negligible. The system is quasi-adiabatic. The mass and heat balances (Eqs. (3) and (4)) show that the temperature, the concentration and the pressure responses are proportional. Thus the phase lag is close to zero. When frequency increases again, the effect of mass transfer resistance appears giving a negative phase lag. The phase lag tends towards $-\pi/4$ in case of pure Fickian diffusion and towards $-\pi/2$ in case of pure surface barrier resistance. Thus it is easy to know the dominant mass transfer resistance.

In the case of bidispersed adsorbent particles (pellets formed by agglomeration of adsorbent microparticules) three new resistances appear: macroporous diffusion resistance, surface barrier at the pellet surface and resistance to heat conduction inside the particle, i.e., in which temperature is not uniform. These resistances induce new characteristic times: $\tau_{D_p}$, $\tau_{sp}$ and $\tau_\lambda$ respectively. The mathematical expressions of the different characteristic times are given in Bourdin et al (1996a).

Figure 3 shows a typical characteristic function obtained with pellets. At low frequency, the characteristic time of heat exchange between the sample and its surroundings is small compared to the volume modulation period. Consequently, the thermal response amplitude is close to zero. When the frequency increases the thermal response increases and tends towards a limit corresponding to the adiabatic behaviour. The out-of-phase function reaches its maximum at an angular frequency close to $1/\tau_h$. For higher frequencies the thermal response decreases due to the macroporous mass transfer resistances which reduce the adsorbed amount during a cycle.

The depths of penetration, $L_T$ and $L_M$, of the thermal and mass waves respectively, are:

$$L_T = \sqrt{\frac{2K}{\omega}} \tag{15}$$

$$L_M = \sqrt{\frac{2D_p}{\omega}} \tag{16}$$

where $\kappa$ is the thermal diffusivity of the pellet and $D_p$ is the macroporous diffusion coefficient. $L_T$ is always larger than $L_M$. At low frequencies, $L_T > L_M > R_p$. The effective heat capacity and the effective adsorbing capacity are independent of the frequency. In that "low frequency" domain the response depends only on the external heat exchange, $h$. When the frequency increases, $L_M$ becomes smaller than $R_P$, and the adsorbing capacity decreases, leading to a decrease of the temperature response. In that frequency domain the temperature response depends only on $D_p$. With a further increase of the frequency, $L_T$ also becomes smaller than $R_p$ and the ratio of the effective adsorbing capacity and the effective heat capacity remains

approximately constant. Thus the temperature response is only slightly dependent on the frequency. This frequency domain allows one to identify the thermal conductivity, $\lambda$, of the pellet. In the "high frequency" domain, the response depends mainly on the crystals at the surface of the pellet, and the final decrease of the temperature response depends on the nanoporous mass transfer resistance. Thus, the measurement of the surface temperature by the infrared detector permits us to determine in a single experiment the mass transfer resistances at both nanoporous and macroporous levels.

## Effect of the Non-Isothermal Compression of the Gas

At low frequency the heat transferred to the gas by the bellows compression/decompression is completely released to the walls during a period. Thus, the gas may be considered isothermal. But when the frequency increases, the gas can no longer be considered isothermal. The major consequence is that some heat is transferred from the gas to the sample during a period, leading to a temperature response even for a non-adsorbing sample. The frequency beyond which this spurious temperature response becomes not negligible depends on the pressure and the thermodynamic properties of the gas.

It can be shown that the maximum amplitude of the temperature response due to this effect is roughly proportional to the product $P \times (\gamma - 1)$ where $\gamma$ is the ratio $C_P/C_V$ of the gas. Therefore, this effect is smaller at low pressure, and smaller for complex molecules having high isochorous heat capacities $C_V$. Figure 4 shows

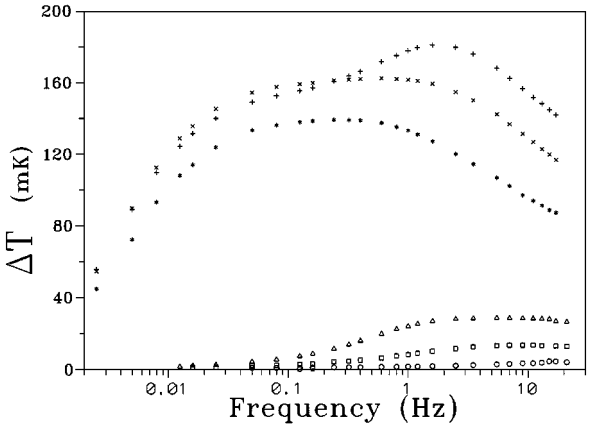


*Figure 4.* Characteristic function amplitude obtained at different pressures of $CO_2$ on NaX crystals and carborandum particles respectively. (∗), (×): 1 kPa. (○), (□): 4 kPa. (Δ), (◊): 10 kPa.

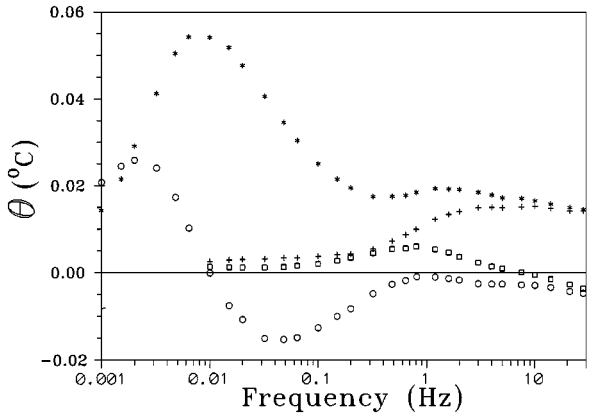


*Figure 5.* Characteristic functions at 9 kPa $CO_2$ of 4A (adsorbent) and 3A (non-adsorbent) pellets respectively: (∗), (+): in-phase functions. (○), (□): out-of-phase functions. The shoulder appearing on the 4A response at about 1 Hz is entirely due to the gas heating effect.

the responses obtained at various pressures with carbon dioxide on NaX crystals and carborundum particles. In fact experiments show that the gas heating effect is always negligible at pressures less than 1 kPa.

If non adsorbent particles of the same geometry and thermal properties as the particles under study are available, it is possible to perform a blank experiment. Figure 5 shows the responses obtained with carbon dioxide at 9 kPa on 4A pellets (adsorbent) and similar 3A pellets (non-adsorbent). One can see that the response of 4A pellets at high frequency is entirely due to the gas heating effect.

This phenomenon has been fully modeled for a spherical sample and a spherical chamber. Unfortunately, this simple model does not give consistent results. It has not been possible to obtain with the same geometrical parameters a nice fit for both pressure and temperature. This failure is probably a consequence of the complex geometry of the actual chamber which is not taken into account by the model.

## Examples of Results

### *Silicalite I-Propane*

Experiments have been performed with silicalite I large crystals ($120 \times 120 \times 350$ $\mu m^3$) provided by O. Talu from Cleveland State University. The crystals were carefully activated under vacuum ($P < 10^{-3}$ Pa) up to 670 K. Reproducible kinetics have been obtained only after several activation cycles, the first measurements

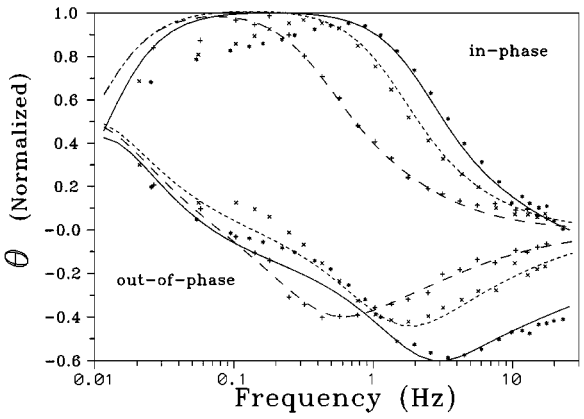


*Figure 6.* Experimental characteristic functions of Silicalite I-Propane for a loading of about 0.5 molecule per cavity (dots) and the corresponding calculated functions (lines). (+), (– – –): 276 K. (×), (---): 301 K. (∗), (–): 334 K.

gave much slower kinetics than the last ones. Figure 6 shows the results obtained for a loading close to 0.5 molecule per cavity at 3 temperatures, and Table 1 gives the experimental conditions and the results obtained by curve fitting. All experimental functions are well fitted by a pure diffusion model and no surface barrier has been observed. Diffusion in the $z$ direction has been neglected because the diffusivity in this direction is at least 4 times slower than in the $xy$ plane. Moreover the concentration gradient is smaller in this direction because the crystal dimension is larger (350 $\mu$m). The diffusivities obtained are mainly averaged over the $x$ zigzag channel direction, and $y$-straight channel direction, and can be compared to the diffusivity $D_{xy}$ as quoted by Talu et al. (1998). Thus, the model used to fit the experimental data assumes a cylindrical geometry with a radius of 60 $\mu$m.

*Table 1.* Experimental conditions and identified diffusivities for Silicalite I-Propane system.

| No. | $P_0$ (Pa) | $T_0$ (K) | $q$ (mol/cav) | $D_c$ ($10^{-9}$ m$^2$ s$^{-1}$) | $\partial \ln q / \partial \ln P$ | $D_0$ ($10^{-9}$ m$^2$ s$^{-1}$) |
|---|---|---|---|---|---|---|
| I | 18 | 276 | 0.4 | 1.8 | 0.93 | 1.7 |
| II | 100 | 301 | 0.4 | 6.1 | 0.81 | 4.9 |
| III | 995 | 334 | 0.6 | 13 | 0.71 | 9.2 |

$D_c$: Transport diffusivity; $D_0$: Corrected diffusivity.

As in these experimental conditions Darken's correction is small, the identified transport diffusivities are close to the self diffusivities. Figure 7 compares the results of the present work with the results obtained with various methods at low adsorbate concentration. These results are interpolated at the same temperature (∼300 K) from the data compiled by Talu et al. (1998)

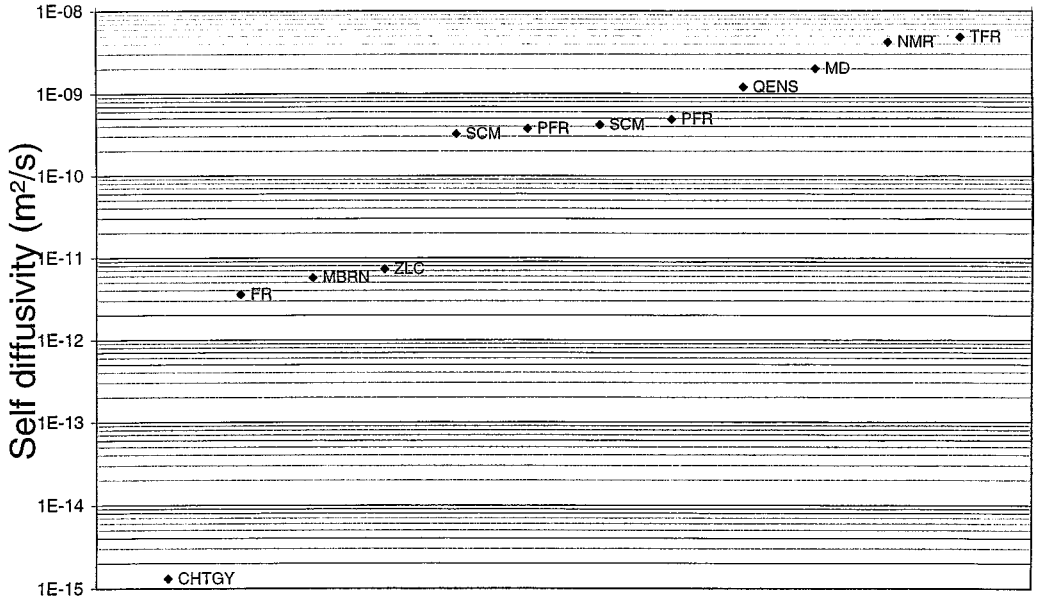


*Figure 7.* Self diffusivities obtained with various methods on, interpolated at 300 K. CHTGY: Chromatography; FR and PFR: Pressure Frequency Response; MBRN: Membrane; ZLC: Zero Length Column; SCM: Single Crystal Membrane; QENS: Quasi Elastic Neutron Scattering; MD: Molecular Dynamics (Talu et al., 1998); NMR: Nuclear Magnetic Resonance (Caro et al., 1985); TFR: Thermal Frequency Response (this work).

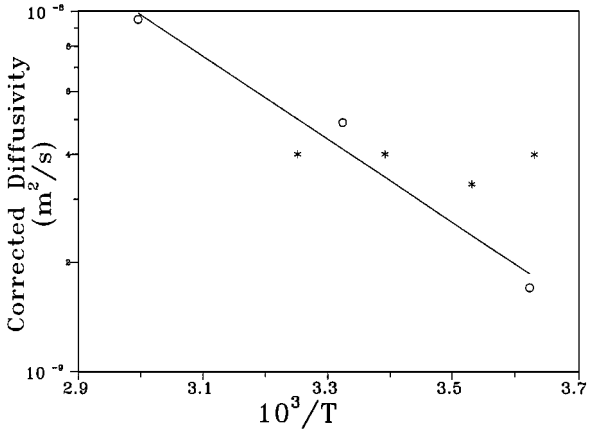


*Figure 8.* Arrhenius plot of the corrected diffusivities of Silicalite I-Propane. (○): this work. The best linear regression gives an activation energy of 20 kJ/mole. (∗): NMR data (Caro et al., 1985) at the same loading (0.5 mol/cav).

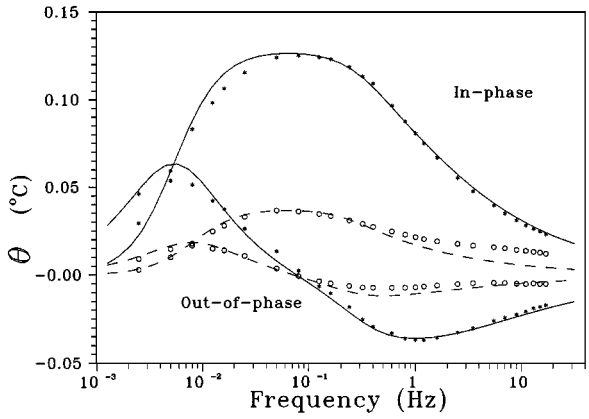


*Figure 9.* Experimental (dots) and calculated (lines) characteristic functions of the NaX-Carbon dioxide system at 95 Pa and 302 K. (∗), (—): anhydrous sample; (○), (− − −): 2.4% hydrated sample.

excep for the NMR whose results come from Caro et al. (1985). One can observe very large inconsistencies between the different techniques. The TFR results agree well with the microscopic methods and the molecular dynamic simulation proving the absence of experimental artefact. In many macroscopic methods, unduly neglected extraneous transfer resistances such as thermal effect or bed effect could strongly affect the results.

Figure 8 shows the Arrhenius plot of the self diffusivities obtained by the TFR method and some results obtained by NMR at 0.5 molecule per cavity (Caro et al., 1985). The activation energy given by the TFR method ($20 \pm 10$ kJ/mol) is much higher than the value given by Heink et al. (1992) (10 kJ/mol) and Eic and Ruthven (1989) (13 kJ/mol). It may be observed that such a discrepancy between Frequency Response and NMR methods has been observed on the activation energies of the NaX-water system (Bourdin et al., 1996c) and also for the silicalite I-$CO_2$ system (Shen and Rees, 1994).

### *NaX-Carbon Dioxide*

The kinetics of the NaX-$CO_2$ system has been studied. The experiments have been performed on 75 $\mu$m edge NaX crystallites, synthesized by H. Kessler ("Laboratoire des Matériaux Minéraux"-ENSC Mulhouse). The crystals were activated in the same way as previously described.

Figure 9 shows the results obtained at 95 Pa and 302 K and Table 2 gives the experimental conditions and the results of the curve fitting for 3 loadings. The experiment with the anhydrous sample can be well fitted with a pure diffusion model and no surface barrier

*Table 2.* Experimental conditions and identified diffusivities for NaX-$CO_2$ system.

| No. | State | $P_0$ (Pa) | $T_0$ (K) | $q$ (mol/cav) | $D_c$ ($10^{-10}$ m$^2$ s$^{-1}$) | $\partial \ln q/\partial \ln P$ | $D_0$ ($10^{-10}$ m$^2$ s$^{-1}$) |
|---|---|---|---|---|---|---|---|
| Ia | Anhydrous | 96 | 302 | 0.9 | 3.4 | 0.77 | 2.6 |
| Ih | Hydrated | 94 | ≪ ≫ | 0.5 | 2.7 | 0.48 | 1.3 |
| IIa | Anhydrous | 410 | ≪ ≫ | 2.0 | 13 | 0.48 | 6.1 |
| IIh | Hydrated | 400 | ≪ ≫ | 1.2 | 6.0 | 0.40 | 2.4 |
| IIIa | Anhydrous | 950 | ≪ ≫ | 3.7 | 43 | 0.24 | 10.5 (∼15)[a] |
| IIIh | Hydrated | 950 | ≪ ≫ | 2.3 | 23 | 0.26 | 6.1 |

[a]NMR result at a loading comprised between 3 and 4 molecules per cavity (Kärger et al., 1993).
$D_c$: Transport diffusivity; $D_0$: Corrected diffusivity.

is observed. One can see that for this system, as well as for the silicalite-propane system, the results agree well with NMR.

In order to study the influence of water on the kinetics, the anhydrous sample was hydrated to a water loading of 2.4% by weight. At this loading, the equilibrium vapor pressure is less than 0.1 Pa. After the water loading, the experiment was performed in the same conditions as those used with the anhydrous sample. A large diminution of the thermal amplitude and a shift of the curves towards the low frequencies can be observed on Fig. 9. One can see that a single component model cannot account for the high frequency part of the spectrum. In spite of the very low water partial pressure, a correct interpretation of these observations might involve partial water desorption accompanying carbon dioxide adsorption. Nevertheless, the curve fitting allows us to determine an approximate diffusivity given in Table 2. One can see that 2.4% water induces a slowing of the kinetics by a factor of about 2.

## Conclusion

The thermal frequency response method using IR detection to measure the temperature of the sample appears to be a powerful method to determine adsorption kinetics parameters in adsorbents and especially in mono or bidispersed samples of zeolite. Unlike conventional sorption rate measurements, this method is not limited to isothermal or quasi-isothermal conditions. This method permits clear separation between the surface transfer processes and the diffusion processes, and in many cases separation between the resistances at the macro and nano scales of an agglomerated adsorbent. The influence of each resistance on the experimental signal appears in a specific frequency window corresponding to its characteristic time. Moreover, the very low overall measurable time constant ($\sim$1 ms) allows us to determine fast kinetic parameters, and permits to compare the results with the results given by microscopic methods.

The method is limited by the heating of the sample due to the non isothermal compression of the gas. This effect is always negligible for pressures smaller than 1 kPa.

Experiments performed on silicalite-propane and NaX-Carbon dioxide show excellent agreement with the microscopic methods, especially with NMR. Moreover it has been shown that a small amount of water in NaX crytals induces a slight slowing of the adsorption kinetics of carbon dioxide.

## Nomenclature

| | | |
|---|---|---|
| $A_P$ | Pressure amplitude | Pa |
| $A_T$ | Temperature amplitude | K |
| $C_s$ | Sample heat capacity | J m$^{-3}$K$^{-1}$ |
| $D_c$ | Transport diffusivity | m$^2$ s$-1$ |
| $D_0$ | Self-diffusivity | m$^2$ s$^{-1}$ |
| $h$ | Heat transfer coefficient | W m$^{-2}$ K$^{-1}$ |
| $K_P$ | Isotherm derivative: $(\partial q/\partial P)_T$ | kg m$^{-3}$ Pa$^{-1}$ |
| $K_T$ | Isobar derivative: $(\partial q/\partial T)_P$ | kg m$^{-3}$ K$^{-1}$ |
| $k_s$ | Surface barrier coefficient | ms$^{-1}$ |
| $P$, $P_e$ | Pressure, its mean value | Pa |
| $q$, $q_e$ | Adsorbed amount its mean value | kg m$^{-3}$ |
| $R$ | Gas constant | J kg$^{-1}$ K$^{-1}$ |
| $R_c$ | Crystal radius | m |
| $r_c$ | Current crystal radius | m |
| $T$, $T_e$ | Temperature, its mean value | K |
| $V$ | Chamber volume | m$^3$ |
| $V_s$ | Sample volume | m$^3$ |
| $v$ | Relative volume amplitude | |
| $\gamma$ | Heat capacity ratio | $C_P/C_V$ |
| $\gamma$ | Non-isothermality coefficient | $\lvert\Delta H\rvert K_T/C_s$ |
| $\Delta H$ | Sorption Enthalpy | J kg$^{-1}$ |
| $\varphi$ | Phase lag | |
| $\sigma$ | Geometrical factor (0, 1 or 2) | |
| $\tau_D$ | Diffusion characteristic time | s |
| $\tau_h$ | Heat transfer characteristic time | s |
| $\tau_s$ | Surface barrier characteristic time | s |
| $\omega$ | Angular frequency | s$^{-1}$ |

## Acknowledgment

We are grateful to professor H. Kessler of the "Laboratoire des Matériaux Minéraux-Ecole Nationale Supérieure de Chimie-Mulhouse" for providing large NaX zeolite crystals, and to professor O. Talu, Cleveland State University, for providing large silicalite crystals.

## References

Bourdin, V., Ph. Grenier, F. Meunier, and L.M. Sun, "Thermal Frequency Response Method for the Study of Mass Transfer Kinetics in Adsorbents," *AIChE J.*, **42** (3), 700–712 (1996a).

Bourdin, V., L.M. Sun, Ph. Grenier, and F. Meunier, "Analysis of the Temperature Frequency Response for Diffusion in Crystals and Biporous Pellets," *Chem. Eng. Sci.*, **51** (2), 269–280 (1996b).

Bourdin, V., A. Germanus, Ph. Grenier, and J. Kärger, "Application of the Thermal Frequency Response Method and of Pulsed Field Gradient N.M.R. to Study Water Diffusion in Zeolite NaX," *Adsorption*, **2**, 205–216 (1996c).

Caro, J., M. Bülow, W. Schirmer, J. Kärger, W. Heink, and H. Pfeifer, "Microdynamics of Methane, Ethane and Propane in ZSM-5 Type Zeolites," *J. Chem. Soc. Faraday Trans. I*, **81**, 2541–2550 (1985).

Do, D.D., *AIChE J.*, **35** (4), 649 (1989).

Eic, M. and D.M. Ruthven, "Intracrystalline Diffusion of Linear Paraffins and Benzene in Silicalite Studied by the ZLC Method," *Zeolites: Facts, Figures, Future*, P.A. Jacobs and R.A. van Santen (Eds.), pp. 897–905, Elsevier Science B.V., Amsterdam, 1989.

Heink, W., J. Kärger, and H. Pfeifer, "High Temperature Pulsed Field Gradient Nuclear Resonance Self-diffusion Measurement of *n*-Alkanes in MFI-Type Zeolite Crystallites," *J. Chem. Soc. Faraday Trans. I*, **88** (23), 3505 (1992).

Kärger, J. and D.M. Ruthven, "On the Comparison Between Macroscopic and NMR Measurements of Intracrystalline Diffusion in Zeolites," *Zeolites*, **9**, 267–281 (1989).

Kärger, J. and D.M. Ruthven, *Diffusion in Zeolites*, pp. 513–525, John Wiley and Sons, New York, 1992.

Kärger J., H. Pfeifer, F. Stallmach, N.N. Feoktistova, and S.P. Zhdanov, "$^{129}$Xe and $^{13}$C PFG NMR Study of the Intracrystalline Self-Diffusion of Xe, $CO_2$ and CO," *Zeolites*, **13**, 50–55 (1993).

Kocirik M., A. Zikanova, P. Struve, and M. Bülow, "Pecularities of the Mass Transport Across Zeolite Crystal Surface," *Z. Phys. Chemie. Leipzig*, **271** (1), 43–50 (1990).

Ruckenstein E., A.S. Vaidyanathan, and G.R. Youngquist, *Chem. Eng. Sci.*, **26**, 1305 (1971).

Ruthven D.M., L.K. Lee, and H. Yucel, "Kinetics of Non-Isothermal Sorption in Molecular Sieve Crystals," *AIChE J.*, **26** (1), 16–23 (1980).

Shen, D and L.V.C. Rees, "Frequency Response Stydy of Single-file Diffusion in Theta 1," *J. Chem. Soc. Faraday Trans. I*, **90** (19), 3017–3022 (1994).

Sun L.M. and F. Meunier, "A Detailed Model for Non-isothermal Sorption in Porous Adsorbents," *Chem. Eng. Sci.*, **42** (7), 1585 (1987).

Talu O., M.S. Sun, and D.B. Shah, "Diffusivities of *n*-Alkanes in Silicalite by Steady-State Single-Crystal Membrane Technique," *AIChE J.*, **44** (3), 681–694 (1998).

Van-den-Begin N.G. and L.V.C. Rees, "Diffusion of Hydrocarbons in Silicalite Using a Frequency Response Method," *Zeolites: Facts, Figures, Future*, P.A. Jacobs and R.A. van Santen (Eds.), pp. 915–924, Elsevier Science B.V., Amsterdam, 1989.

Zhong G.M., Ph. Grenier, and F. Meunier, "Influence des transferts intergranulaires sur la détermination gravimétrique de la cinétique d'adsorption," *The Chem. Eng. J.*, **53** (147), 147–150 (1993).